



Multigap Resistive Plate Chamber read out by $1 \times 1 \text{ cm}^2$ pads with the NINO ASIC

Z. Liu ^{a,b,*}, D.W. Kim ^c, M.C.S. Williams ^{a,c,d}, A. Zichichi ^{a,d,e}, R. Zuyewski ^{b,e}

^a European Centre for Nuclear Research (CERN), Geneva, Switzerland

^b ICSC World Laboratory, Geneva, Switzerland

^c Gangneung-Wonju National University, Gangneung, South Korea

^d INFN and Dipartimento di Fisica e Astronomia, Università di Bologna, Italy

^e Museo Storico della Fisica e Centro Studi e Ricerche E.Fermi, Roma, Italy

ARTICLE INFO

Keywords:

Multigap Resistive Plate Chamber
 $1 \times 1 \text{ cm}^2$ pad
 Efficiency
 Time resolution

ABSTRACT

The Multigap Resistive Plate Chamber (MRPC) is a possible candidate for the Semi-Digital Hadronic Calorimeter (SDHCAL). Two $4.5 \times 20 \text{ cm}^2$ active area MRPCs have been built to study the time resolution using the NINO ASIC as front-end electronics. The granularity of the active area is provided by a 4×16 array of $1 \times 1 \text{ cm}^2$ pick-up pads. Two different designs have been used for the two chambers: a six gas gap MRPC (6-gap MRPC) with a $220 \mu\text{m}$ gap size and a ten gas gap MRPC (10-gap MRPC) with a $160 \mu\text{m}$ gap size. An efficiency of 95% and 97% has been reached respectively. A time resolution of 50 ps for the 6-gap MRPC and 30 ps for the 10-gap MRPC has been achieved. The multiplicity study of this two MRPCs shows that a large fraction of the single hit is recorded in the events (71% for 6-gap MRPC and 64% for 10-gap MRPC).

1. Introduction

The Multigap Resistive Plate Chamber (MRPC) is a gaseous detector consisting of a stack of resistive plates [1]. Typically it has a time resolution between 30 and 100 ps [2]. Thanks to its very good timing characteristics and inexpensive cost the MRPC is widely used as a Time of Flight (TOF) detector in nuclear and high energy experiments: examples are the ALICE experiment [3,4] and the STAR experiment [5]. In our previous work [6], we have successfully developed a $1 \times 1 \text{ m}^2$ MRPC prototype for the Semi-Digital Hadronic Calorimeter (SDHCAL) that has been proposed for future leptonic collider experiments [7]; the MRPC has a low dark count rate and reached an efficiency of 94%. For that prototype, we used the HARDROC chips [8]: this ASIC is not designed for precise timing measurement, so the time resolution had not been evaluated.

In this paper we have built two MRPCs and focused on their excellent time resolution: timing is a key feature, which can be used for background reduction, vertex determination and to separate overlapping hadronic showers. Moreover, the time resolution of an MRPC with pick-up pad size of $1 \times 1 \text{ m}^2$ has not been reported before; it is important to know whether the timing performance of this configuration can fulfil the requirement (better than 100 ps) of SDHCAL. The NINO ASIC is used as the front-end readout for these two MRPCs; it was developed for the ALICE (A Large Ion Collider Experiment) TOF detector [9]. It is an amplifier/discriminator with low jitter time, which is very suitable

for MRPC timing studies. ALICE TOF MRPCs have pick-up pads with a dimension of $3.5 \times 2.5 \text{ cm}^2$; the global time resolution of this system is 56 ps [4]. The MRPCs we have built in this paper have a $1 \times 1 \text{ cm}^2$ pick-up pad configuration (i.e. much smaller than the pick-up pads of the ALICE TOF MRPCs). This design gives a high granularity that matches the desired segmentation of the SDHCAL. The two MRPCs have been examined in the beam test to check their efficiency, time resolution and multiplicity. Both reach above 95% efficiency as expected. The MRPC with six $220 \mu\text{m}$ gas gaps shows a time resolution of 50 ps and the MRPC with ten $160 \mu\text{m}$ gas gaps shows a time resolution of 30 ps. Details of test result are described below.

2. MRPC with $1 \times 1 \text{ cm}^2$ pads

Two MRPCs with $1 \times 1 \text{ cm}^2$ pick-up pads have been built. One is a six gas gaps MRPC (6-gap MRPC) with a gap size of $220 \mu\text{m}$. The 6-gap MRPC consists of 2 external glass plates and 5 inner glass plates. The other MRPC has ten gaps (10-gap MRPC) with a gap size of $160 \mu\text{m}$. The structure of the 10-gap MRPC is similar to the 6-gap MRPC. It has 9 inner glass plates instead of 5 inner glass plates. The cross section of an edge of the 6-gap MRPC is shown in Fig. 1. The thickness of all glass plates is 0.28 mm with a bulk resistivity of $1.3 \times 10^{12} \Omega \text{ cm}$ at $24 \text{ }^\circ\text{C}$. The outer surface of the external glass sheets has been coated with a resistive paint of $5 \text{ M}\Omega/\square$; the high voltage is applied to these resistive electrodes. The external glass plates of the two MRPCs have a dimension

* Corresponding author.

E-mail address: zheng.liu@cern.ch (Z. Liu).

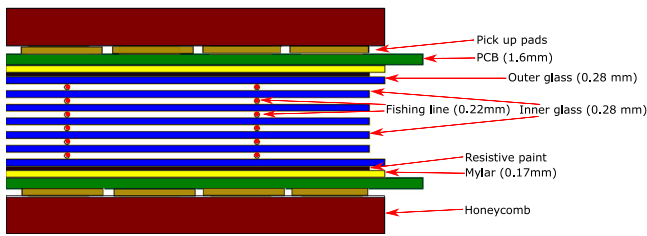


Fig. 1. Cross section view of the 6-gap MRPC.

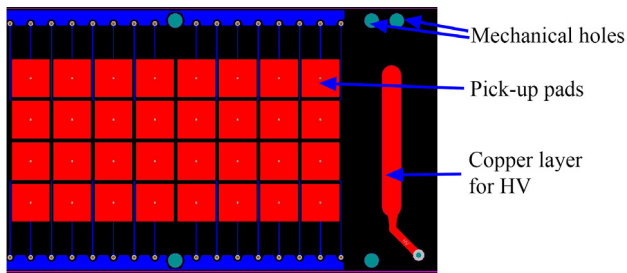


Fig. 2. A partial view of pick-up pads (4×8 pads) design PCB layout. Plastic screws for fishing lines are fixed through the mechanical holes. The copper plane is used to apply high voltage.

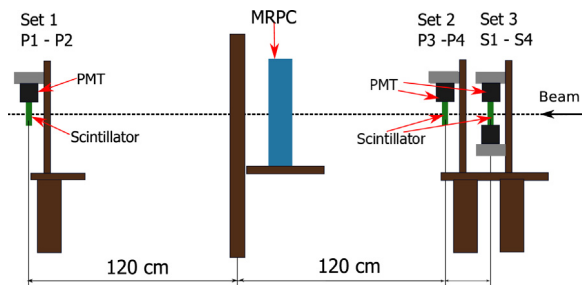


Fig. 3. The experiment setup for the MRPC test at the T10 test beam facility.

of $6 \times 24 \text{ cm}^2$ with a $4.5 \times 20 \text{ cm}^2$ voltage electrode; the inner glass plates have a dimension of $5 \times 20 \text{ cm}^2$. Nylon fishing lines with a diameter of $220 \mu\text{m}$ and $160 \mu\text{m}$ are used as spacers to define the gas gaps of the 6-gap MRPC and the 10-gap MRPC respectively. The fishing lines are routed across the surface of the glass from one side to the other and fixed with plastic screws at both sides of the Printed Circuit Board (PCB). A mylar sheet of 0.17 mm is placed between the electrode and the PCB to isolate the high voltage. The PCBs of 1.6 mm thickness are placed between the mylar and the honeycomb panels. The pick-up pads are etched on one side of the PCB. The dimension of the pick-up pad is $1 \times 1 \text{ cm}^2$ with a 1 mm gap between pads. The pads located on the PCB are an array of 4×16 . Fig. 2 shows a partial view (only 4×8 pads) of the pick-up pad design in the PCB layout. Two honeycomb panels are attached to the top and bottom layer of MRPC for mechanical support; the complete MRPC is mounted inside a gas-tight aluminium box. The signals from the paired pick-up pads on the top and bottom PCB form a differential signal discriminated by the NINO ASIC and readout by WaveCatcher [10].

3. Experiment setup

The two MRPCs were tested in the T10 test beam facility at CERN [11]. Fig. 3 shows a schematic drawing of the experimental setup. The beam was mainly composed of negative pions with $5 \text{ GeV}/c$ momentum. All the chambers are filled with a gas mixture of $95\% \text{ C}_2\text{H}_2\text{F}_4$ and $5\% \text{ SF}_6$. Three scintillator sets were well aligned with respect to the beam-line; the logic AND of signals from the scintillators

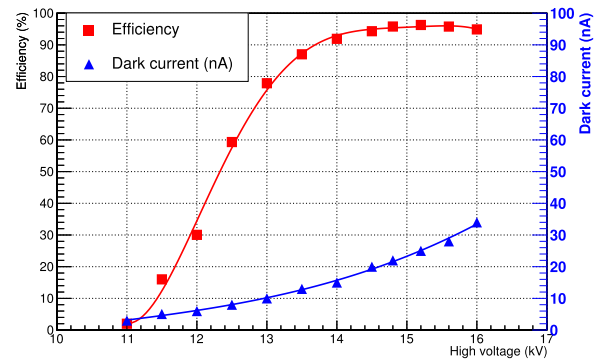


Fig. 4. The efficiency and dark current of the 6-gap MRPC for various applied voltages. The error bars are contained in the size of the symbols; the lines are to guide the eye.

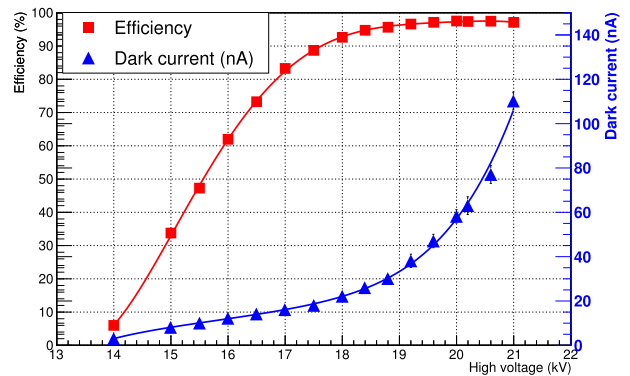


Fig. 5. The efficiency and dark current of the 10-gap MRPC for various applied voltages. The error bars are contained in the size of the symbols; the lines are to guide the eye.

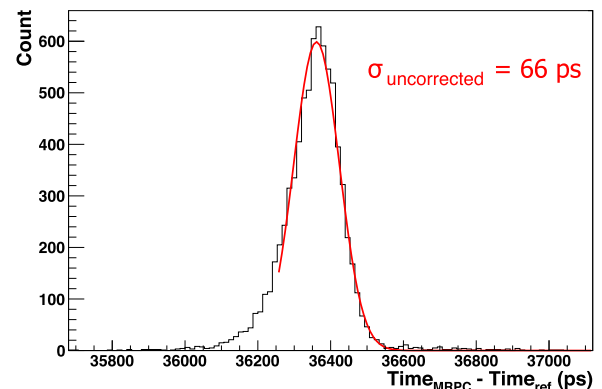


Fig. 6. Time difference between the 6-gap MRPC and the time reference without slewing correction. The applied voltage is 15.6 kV and the NINO threshold is 170 mV .

sets create the trigger signal to the DAQ system. Scintillator set 1 and set 2 defines an area of the beam of $1.2 \times 1.2 \text{ cm}^2$, which allows us to select one of the $1 \times 1 \text{ cm}^2$ pads to study. Scintillator set 3 consists of two orthogonal scintillator bars with dimension of $2 \times 2 \times 20 \text{ cm}^3$. Each end ($2 \times 2 \text{ cm}^2$) of each bar is coupled to a PMT (S1 and S2 for one bar, S3 and S4 for the other bar). The average hit time of these four PMTs (S1–S4) are used also as a time reference and gives a time resolution (sigma) of $35.0 \pm 0.7 \text{ ps}$ [12]. The MRPCs were mounted on an X–Y moving table between Set 1 and Set 2. This table could be moved with a step of 0.1 mm . A position scan of the pads was done. By checking the hit distribution of each pad, we are able to centre the beam in the middle of one pad of the MRPC.

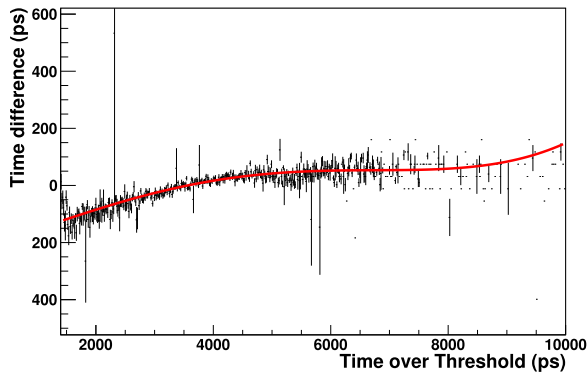


Fig. 7. Time difference between the 6-gap MRPC and the time reference shown as a function of the pulse width. The applied voltage is 15.6 kV and the NINO threshold is 170 mV.

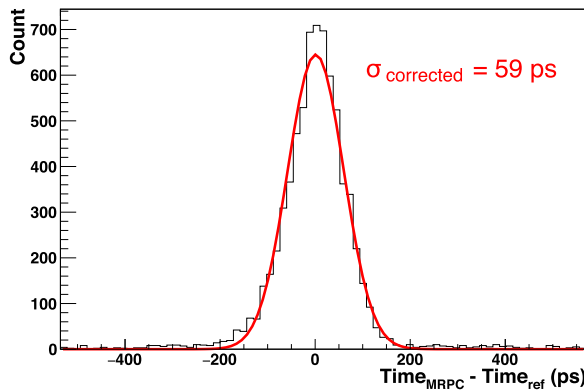


Fig. 8. Time difference between the 6-gap MRPC and the time reference after slewing correction. The applied voltage is 15.6 kV and the NINO threshold is 170 mV.

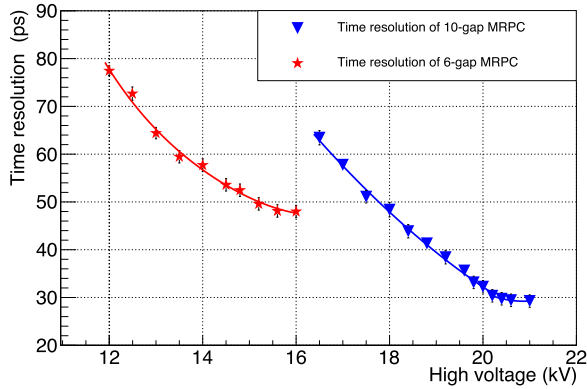


Fig. 9. The time resolution of MRPCs as a function of different voltages. The lines are to guide the eye.

4. Results

The two MRPCs have been tested with an instantaneous flux of 2 kHz/cm². The instantaneous flux of particles is measured by counting the number of coincidences of set 1 and set 2 during the 360 ms spill period. Fig. 4 shows the efficiency and dark current of the 6-gap MRPC under different voltages (between 11 kV and 16 kV); the NINO threshold is fixed at 170 mV.¹ The efficiency of 6-gap MRPC reaches a plateau of

¹ The threshold value quoted is the differential voltage applied to the NINO threshold pins. For signals from the MRPC a 4 mV NINO threshold is equivalent to a signal of 1 fC.

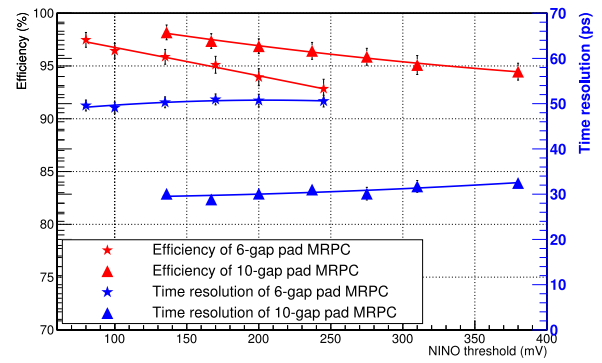


Fig. 10. The efficiency and time resolution of the MRPCs at different NINO threshold values. The lines are to guide the eye.

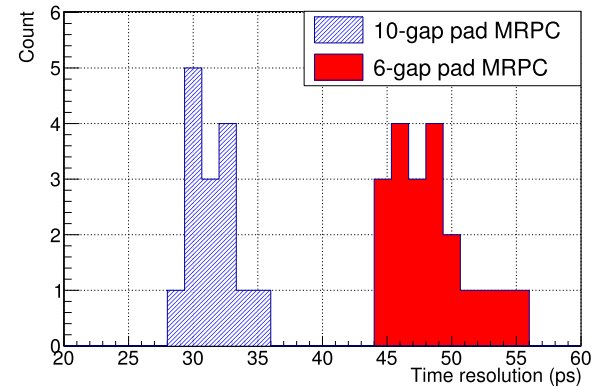


Fig. 11. Time resolution histogram of the 6-gap MRPC and the 10-gap MRPC.

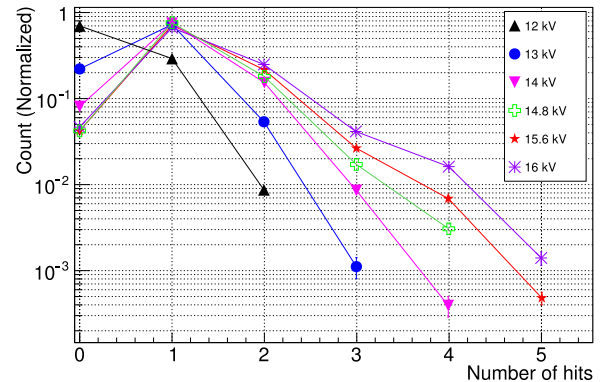


Fig. 12. Multiplicity plot of the 6-gap MRPC at different voltages. The NINO threshold is fixed at 170 mV.

95% at 14.8 kV as we expected. The dark current for the full active area is below 20 nA when the applied voltage is below 14 kV and increases to 34 nA when the applied voltage is 16 kV. Fig. 5 shows the efficiency curve for the 10-gap MRPC at different voltages with a NINO threshold of 170 mV. The efficiency of 10-gap MRPC reaches a plateau of 97% at 19.6 kV. This good efficiency value and long plateau allow us to set a safe operation voltage with good performance.

The hit time of each pad of MRPC is determined by the differential signals from paired pads (cathode and anode pick-up pads) on the top and bottom PCB. The MRPC time is represented by the hit time of the pad centred with the beam spot. Fig. 6 shows a typical histogram of the time difference between the 6-gap MRPC and the reference time. A time resolution of 66.0 ± 0.8 ps is measured by fitting a Gaussian. These measurements need to be corrected for the time slewing effect,

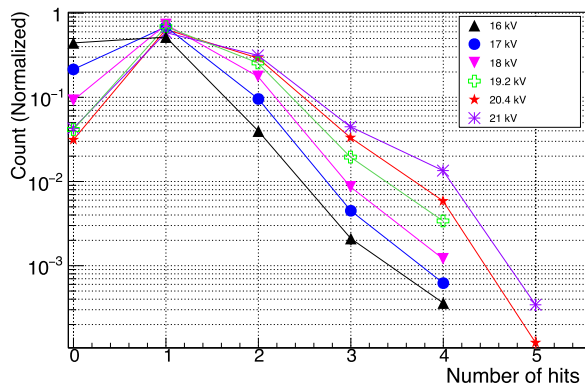


Fig. 13. Multiplicity plot of the 10-gap MRPC at different voltages. The NINO threshold is fixed at 170 mV.

necessary since the NINO chip is a fixed threshold discriminator. The output pulse width of the NINO varies according to the input charge (Time over Threshold, ToT); thus we can use the ToT information to correct the time measurements. In Fig. 7 the correlation between the ToT and the time signal of a pad of the 6-gap MRPC is shown; this profile is fitted with a fourth order polynomial function for the slewing correction. In Fig. 8 the time difference between the 6-gap MRPC and the reference time after slewing correction is shown. The time distribution has been fitted using a Gaussian function; a time resolution of 59.0 ± 0.7 ps has been reached. The final time resolution, after subtracting the jitter of the PMTs time reference, is $\sqrt{59^2 - 35^2} = 48.0 \pm 1.0$ ps.

In Fig. 9 the time resolution of the two MRPCs for different voltages is shown. The time resolution improves with a higher voltage applied for both MRPCs. Between 14.8 kV and 16 kV, the 6-gap MRPC has a time resolution better than 50 ps. The time resolution of the 10-gap MRPC reaches 30 ps between the voltage values of 20.2 kV and 21 kV.

The performance of the two MRPCs at different NINO threshold values has been also examined. Note: The value of threshold quoted here is the differential voltage applied to the NINO threshold pins; a threshold value of 4 mV corresponds to an input signal threshold of 1 fC (170 mV sets the threshold at 42.5 fC). In Fig. 10 the efficiency and time resolution versus the NINO threshold are reported. The voltage of the 6-gap MRPC is fixed at 15.6 kV and that of the 10-gap MRPC at 20.4 kV. The efficiency of the 6-gap MRPC reaches 97% at an 80 mV threshold value and drops to 93% when the threshold is set at 245 mV. The time resolution is almost flat for NINO thresholds between 80 mV and 245 mV. The 10-gap MRPC has a similar trend. Its efficiency decreases from 98% to 94% when the NINO threshold is increased from 135 mV to 380 mV. Within this NINO threshold range, there is only a small reduction of the time resolution.

The two MRPCs have been moved to different X–Y positions to check the timing performance for different pads. The voltage of the 6-gap MRPC was fixed at 15.6 kV and that of the 10-gap MRPC was at 20.4 kV. For both MRPCs the NINO threshold was set at 170 mV. The time resolution distribution of the pads of the two MRPCs are shown in Fig. 11. 20 pads of the 6-gap MRPC have been examined. The best time resolution we obtained was around 45 ps and 70% of the pads had a time resolution better than 50 ps. 16 pads of the 10-gap MRPC have been tested, the best time resolution is around 28 ps and most of the pads have a time resolution between 30 to 33 ps. For both MRPCs, the variation of time resolution between different pads is quite small.

A multiplicity distribution of MRPC shows the number of pads fired by a single particle passing through the MRPC. A plot of the multiplicity distribution for the 6-gap MRPC is shown in Fig. 12. The mean value

of the number of hits increases with higher voltage. At the voltage of 15.6 kV (95% efficiency), the 71% of the events record a single hit. In Fig. 13 a multiplicity plot also for the 10-gap MRPC is reported. The trend is similar to that of the 6-gap MRPC. At the voltage of 20.4 kV (97% efficiency), the 64% of the events recorded a single hit (a lower value than that of the 6-gap MRPC). A large fraction of single hits on the pad is desired since the SDHCAL uses the number of tracks in the event to reconstruct the energy deposit.

5. Summary and discussion

Two 4.5×20 cm² active area MRPCs with 64 pick-up pads of 1×1 cm² each have been successfully operated and tested in a beam facility. The efficiency of the 6-gap MRPC reaches 95% when the voltage is higher than 14.8 kV. This MRPC also shows a good time resolution of 50 ps and has a low crosstalk between pads. The 50 ps time resolution is better than the similar configuration MRPC with pad readout or strip readout that gives time resolution of 60 to 70 ps [5,12]. The good performance of this 6-gap MRPC meet the requirements of SDHCAL detector plans (The time resolution of timing layer should be better than 100 ps).

The efficiency of 10-gap MRPC reaches 97% at 20.4 kV. Thanks to a narrower gas gaps (the 6-gap MRPC has a gap size of 220 μ m) of 160 μ m, it has an excellent time resolution of 30 ps, which is better than the 50 ps of 6-gap MRPC. A MRPC consisting of 24 gaps with 2.45×7.4 cm² pick-up strips reported in [13] achieves 20 ps, which is better than the 10-gap MRPC. However, the 10-gap MRPC has fewer gas gaps and it is read out with 1×1 cm² pick-up pads. It has a high granularity and 30 ps time resolution together with a simply and compact design.

Acknowledgements

The results presented here were obtained at the T10 test beam in the east hall at CERN. The authors acknowledge the support received by the operators of the PS.

References

- [1] E. Cerron Zeballos, et al., A new type of resistive plate chamber: the multigap RPC, Nucl. Instrum. Methods Phys. Res. A 374 (1996) 132–135.
- [2] A. Akimov, et al., The multigap resistive plate chamber as a time-of-flight detector, Nucl. Instrum. Methods Phys. Res. A 456 (1) (2000) 16–22.
- [3] Alice Collaboration, Performance of the alice experiment at the CERN LHC, Internat. J. Modern Phys. A 29 (24) (2014) 143004.
- [4] N. Jacazio, PID performance of the alice-tof detector in run 2, 2018, arXiv preprint arXiv:1809.00574.
- [5] W.J. Llope, S.T.A.R. Collaboration, STAR Collaboration, Multigap rpcs in the star experiment at rhic, Nucl. Instrum. Methods Phys. Res. A 661 (2012) S110–S113.
- [6] F. Carnesecchi, et al., Performance study of a large 1×1 m² MRPC with 1×1 cm² readout pads, Nucl. Instrum. Methods Phys. Res. A 871 (2017) 113–117.
- [7] G. Baulieu, et al., Construction and commissioning of a technological prototype of a high-granularity semi-digital hadronic calorimeter, J. Instrum. 10 (10) (2015) P10039.
- [8] F. Dulucq, et al., HARDROC: Readout chip for CALICE/EUDET digital hadronic calorimeter, in: Nuclear Science Symposium Conference Record, NSS/MIC, 2010 IEEE, IEEE, 2010.
- [9] F. Anghinolfi, et al., NINO: an ultra-fast and low-power front-end amplifier/discriminator ASIC designed for the multigap resistive plate chamber, Nucl. Instrum. Methods Phys. Res. A 533 (1) (2004) 183–187.
- [10] D. Breton, J. Maalmi, E. Delagnes, Using Ultra Fast Analog Memories for Fast Photo-detector Read Out, NDIP 2011, Lyon.
- [11] <http://sba.web.cern.ch/sba/BeamsAndAreas/East/East.htm>.
- [12] Z. Liu, et al., 20 gas gaps Multigap Resistive Plate Chamber: Improved rate capability with excellent time resolution, Nucl. Instrum. Methods Phys. Res. A 908 (2018) 383–387.
- [13] S. An, et al., A 20 ps timing device a multigap resistive plate chamber with 24 gas gaps, Nucl. Instrum. Methods Phys. Res. A 5941 (1) (2008) 39–43.